International Journal of Information, Control and Computer Sciences
ISSN: 2517-9942
Vol:1, No:4, 2007

Region Based Hidden Markov Random Field Model for Brain MR Image Segmentation

Terrence Chen, and Thomas S. Huang

***Abstract*—**In this paper, we present the region based hidden Markov random field model (RBHMRF), which encodes the characteristics of different brain regions into a probabilistic framework for brain MR image segmentation. The recently proposed TV+L^1 model is used for region extraction. By utilizing different spatial characteristics in different brain regions, the RMHMRF model performs beyond the current state-of-the-art method, the hidden Markov random field model (HMRF), which uses identical spatial information throughout the whole brain. Experiments on both real and synthetic 3D MR images show that the segmentation result of the proposed method has higher accuracy compared to existing algorithms.

***Keywords*—**Finite Gaussian mixture model, Hidden Markov random field model, image segmentation, MRI.

I. Introduction

Recent developments in neuroimaging technologies have created unprecedented opportunities to reveal the mysteries of the brain –how i t works and what goes wrong when it is injured or diseased. For example, high-resolution, 3D anatomical information of the brain can now be obtained in a routine manner with magnetic resonance imaging (MRI). However, as the field of functional human brain mapping has matured it has become apparent that a comprehensive understanding of the human brain, and its relationship with cognition, will require a quantitative assessment of individual differences in both brain function and structure. This observation has become increasingly obvious in both neuropathological populations (e.g. multiple sclerosis, schizo-phrenia, Alzheimer's Dementia), as well as normal aged populations. Nevertheless, optimally accurate and efficient methods for characterizing brain structure from medical images remain elusive, and current methods remain imperfect. To assess brain structure, accurate classification of magnetic resonance images according to tissue type at voxel level is needed. Specifically, the global or local morphological features of gray matter (GM), white matter (WM), or cerebrospinal fluid (CSF) are characteristic for describing disease severity or disease entities, and more recently have been linked to individual differences in cognitive performance and brain function, particularly in older adults. Due to the overwhelming amount of data generated to represent each MR image, manual analysis and interpretation of an entire 3D brain MR image is not practical. Therefore, automatic or semi-automatic computer-aided analysis tools are important. Although MR images have higher spatial resolution and better soft-tissue contrast than the other diagnostic imaging modalities, fully automatic segmentation of MR images remains difficult and the results in current literature still have room for improvement. This is due to somewhat noisy MR data caused by time and equipment limitation. In this paper, we propose a novel region based hidden Markov random field approach to quantify brain structure that goes beyond current methods by incorporating an enhanced model of spatial information into a statistical approach to MR image segmentation. The rest of the paper is organized as follows: Section II introduces some existing solutions for brain MR image segmentation. Section III further explains the FGM and the HMRF models. Section IV presents the proposed RBHMRF model. We conduct experiments on both synthetic and real 3D MR images in Section V, followed by the discussion and conclusion in the last section.

T. Chen, is with the Department of Computer Science, University of Illinois at Urbana Champaign, Urbana, IL 61821 USA (e-mail: tchen5@ifp.uiuc.edu).

Prof. T. S. Huang is with the Electrical and Computer Engineering Department, University of Illinois at Urbana Champaign, Urbana, IL 61821 USA (e-mail: huang@ifp.uiuc.edu).

II. Existing Solutions

Several methods have been proposed to segment brain MR images. The methods are either based on the intrinsic structure of the data or based on statistical frameworks. Structural based methods rely on apparent spatial regularities of image structures such as edges [3], and regions [10]. However, the performance is not satisfying when the images are with noise, artifacts, and local variations, which is often the case in real data. Instead, statistical based methods use a probability model to classify the voxels into different tissue types based on the intensity distribution of the image. Methods based on statistical frameworks can be further divided into non-parametric methods or parametric methods.. In non-parametric methods, the density model of the prior relies entirely on the data itself, i.e. the K-nearest-neighbors (K-NN) [7] method. Non-parametric methods are adaptive, but its limitation is the need of a large amount of labeled training data. In contrast, non-parametric methods rely only on the explicit functional form of intensity density function of the MR image. Finite Gaussian mixture (FGM) model [8] and hidden Markov random field (HMRF) model [9] are two representative methods used in this category. We briefly introduce the FGM and the HMRF models in the next section since they are highly

related to the proposed model. We would like to note here that the proposed RBHMRF model is a statistic framework but also with the consideration of intrinsic structures of the data.

III. The FGM and the HMRF Models

We begin with the simpler finite Gaussian mixture (FGM) model. A finite Gaussian mixture model can be represented by a simple graphical model in figure 1 (A). x_i is the ground truth label of a voxel and y_i is the observed intensity of that voxel. Let $\boldsymbol{L}$ denote the set of tissue classes and $\boldsymbol{S}$ denote the set of the voxel index. That is, $\boldsymbol{L} = \{CSF, GM, WM\}$; $\boldsymbol{S} = \{1, 2, \ldots, N\}$. For every $l \in \boldsymbol{L}$ and $i \in \boldsymbol{S}$,

$$P(l) = P(x_i = l) = \omega_l \quad (1)$$

$$p(y_i \mid l) = f(y_i; \theta_l) \quad (2)$$

where $f(y_i;\theta_l) = \frac{1}{\sqrt{2\pi\sigma_l^2}} \exp(-\frac{(y_i - u_l)^2}{2\sigma_l^2})$ in the finite Gaussian mixture model with mean u_l and variance σ_l^2. As a result, let ϕ be the model parameter set, $\phi = \{\omega_l; \theta_l \mid l \in \boldsymbol{L}\}$. The marginal distribution of $y_i = y$ can be obtained by

$$p(y \mid \phi) = \sum_{l \in L} p(l, y \mid \phi) = \sum_{l \in L} p(l) \cdot p(y \mid l) = \sum_{l \in L} p(l) \cdot f(y; \theta_l) \quad (3)$$

The FGM model is mathematically simple and can be computed efficiently. However, no consideration of spatial information becomes its limitation, especially when data is noisy. The segmentation only relies on the intensity histogram of the data and therefore is sensitive to noise and other artifacts or variations. To overcome this limitation, a hidden Markov random field (HMRF) model is derived [9]. The HMRF model is based on the Markov random field (MRF) theory, in which the spatial information is encoded through a neighborhood system. For each voxel x_i, denote x_{N_i} as its neighborhood, which is a set of voxels neighboring x_i, where $x_i \notin x_{N_i}$, $x_i \in x_{N_j} \Leftrightarrow x_j \in x_{N_i}$. Let $\mathbf{x} = (x_1, x_2, \ldots, x_N)$ denote a single configuration. According to the MRF theory,

$$P(\mathbf{x}) > 0 \quad (4)$$

$$P(x_i \mid x_{\boldsymbol{S}-\{i\}}) = P(x_i \mid x_{N_i}) \quad (5)$$

where $\boldsymbol{S}$ denotes index of the whole set of voxels. Based on the Hammersley-Clifford theorem [1],

$$P(\mathbf{x}) = Z^{-1} \exp(-U(\mathbf{x})), \text{ and } U(\mathbf{x}) = \sum_{c \in C} V_c(\mathbf{x}) \quad (6)$$

where Z is a normalizing constant, $U(\mathbf{x})$ is the energy function, and V_c denotes a clique potential.

The intuition behinds the HMRF model is that a voxel is more likely to be of a certain tissue type if the neighboring voxels in are also of that type. Based on this assumption, the clique potential is normally defined as

$$V_c = -\delta(x_i - x_j), \quad \text{where } i \neq j \quad (7)$$

or in similar manner. Finally, a HMRF model with a Gaussian emission distribution can be derived as

$$p(y_i \mid x_{N_i}, \theta) = \sum_{l \in L} f(y_i; \theta_l) p(l \mid x_{N_i}) \quad (8)$$

where $f(y_i; \theta_l)$ is the same as it in (2). The difference between the HMRF model and the FGM model are the term $p(l \mid x_{N_i})$ in (8) and the term $p(l)$ in (3). If we discard the relationship between neighboring voxels, $p(l \mid x_{N_i})$ is the same as $p(l)$. In other words, the only difference between FGM and HMRF model lies in whether the spatial constraint is encoded. Figure 1 (B) illustrates the idea of the HMRF model with a two dimensional first order neighborhood system. Normally, an Expectation-Maximization (EM) algorithm is used to fit both the FGM and the HMRF model. Zhang et. al. [9] incorporated a bias field correction algorithm [5] into the HMRF model and the complete framework can be illustrated by figure 1 (C).

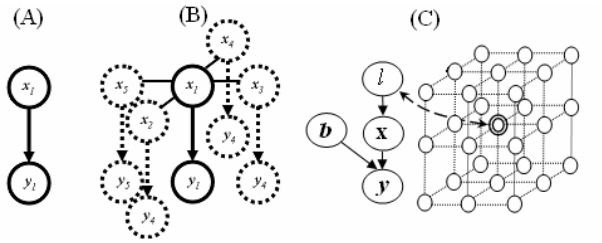

Fig. 1. (A) The FGM model. (B) The HMRF model. (C) The HMRF model with bias field estimation.

IV. The RBHMRF Model

Although HMRF models have yielded relatively better results by taking into account the spatial relationships between neighboring voxels, it is criticized that the improvement of segmentation accuracy is with no significant differences especially in cleaner data but the computation overhead of it is much larger than the FGM model [4]. This can be easily understood because the spatial constraint encoded through the HMRF model is only aiming to solve the data with noise and local variations but not taking the characteristics of human brain structure into account. Therefore, HMRF model treats the probability of a voxel being *WM*, *GM*, or *CSF* all the same. However, we notice that in human brain, *WM* and *CSF* are only adjacent to each other in the regions around the ventricles. In most of the brain regions, *WM* are covered by *GM* and is not adjacent to *CSF* at all. We encode this information into the segmentation framework and propose the region based hidden Markov random field model (RBHMRF).

In the RBHMRF model, the brain is separated into two regions showed in figure 2. Region $\boldsymbol{B}$ contains the voxels surrounding and inside the ventricles while region $\boldsymbol{A}$ includes all the other voxels. The RBHMRF model can also be illustrated by figure 1 (C). Each voxel in an image corresponds to one of the number of classes $x_i = l \in \boldsymbol{L} \equiv \{CSF(0), GM(1), WM(2)\}$which are characterized by an intensity distribution

(i.e. Gaussian distribution). $\boldsymbol{b}$ represents the bias field effect. The probability density of the vector of voxel values $\mathbf{x}$ for the latent image corresponding to class l is $p(\mathbf{x} \mid l) = N(\mu_l, \phi_l)$. μ_l is the mean of the latent image and ϕ_l is the covariance matrix that specifies the variability of each voxel in the latent image. $\mathbf{y}$ is the final observed image. Given the prior image $p(\mathbf{x} \mid l)$, the initial estimation of the bias field $\boldsymbol{b}$, and the observed image $p(\mathbf{y} \mid \boldsymbol{b}, \mathbf{x})$, the posterior distribution $p(l \mid \mathbf{y})$ can be calculated by the MAP estimation of the bias field $p(\boldsymbol{b} \mid \mathbf{y}, \mathbf{x})$ and the $p(\mathbf{x} \mid \mathbf{y}, \boldsymbol{b})$ through the EM algorithm. For fair comparison, we directly apply the method of Guillemaud and Brady [5] to estimate the bias field since it is also used in the HMRF model [9] used to compare with the proposed model.

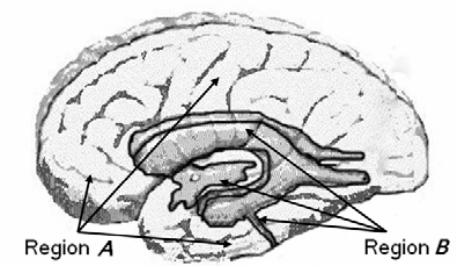

Fig. 2. Region *A* and *B* of the RBHMRF model.

Now we come to the main difference between RBHMRF model and the HMRF model. In the RBHMRF model, different weightings are assigned to the neighborhood system in different brain regions. In the RBHMRF model, the energy function is

$$U(\mathbf{x}) = \sum_{c \in C} V(\mathbf{x}) \tag{9}$$

which is the same as (6). In region $\boldsymbol{B}$, the clique potential is the same as (7), however, in region $\boldsymbol{A}$, the clique potential is modified as

$$V_c = -\delta(x_i - x_j) - \omega \cdot \delta(|x_i - x_j| - 1) \tag{10}$$

where ω is the weighting factor. By this way, a CSF voxel in the neighborhood system can also contribute to the central voxel being a gray matter but not being a white matter, and vice versa. Therefore, this reduces the probability that *WM* and *CSF* are adjacent to each other.

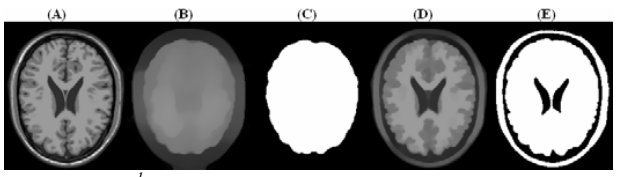

Fig. 3. TV+L^1 model for brain and ventricle extraction. (A) Input brain MR image, f ; (B) u with λ = 0.2; (C) Thresholding on (B) to get brain region; (D) u with λ = 0.6; (E) Thresholding on (D) to get ventricle regions.

A. The TV+L^1 *model with RBHMRF*

One of the issues of the proposed RBHMRF model is to extract the region of the ventricles (region $\boldsymbol{B}$) for different weightings. This can be achieved by the TV+L^1 model [2] defined as:

$$\min_u \int_\Omega |\nabla u(x)| dx \qquad s.t. \|f(x) - u(x)\|_{L^1} \le \sigma, \tag{11}$$

where Ω is the image support and functions f and u are defined on Ω. By changing the only parameter λ, the TV+L^1 model has the capability of selecting different scale objects in u of an image f with very good edge-preserving characteristic. Figure 3 shows how the TV+L^1 model can be used for ventricle regions extraction. The detail of using the TV+L^1 model for ventricles extraction is under another working paper, which is not the main focus here.

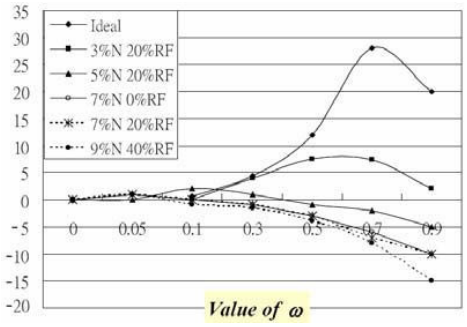

Fig. 4. Improvement ratio (%) of the RBHMRF model to the HMRF model with different values of ω on images with different noise and bias field levels.

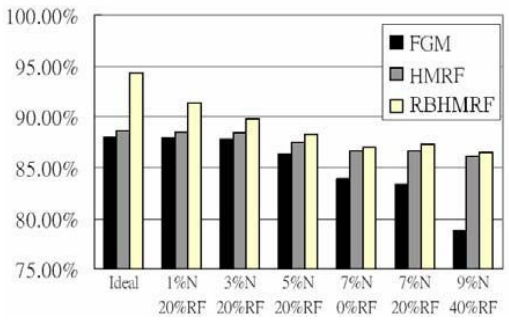

Fig. 5. Comparison of the percentages of correctly classified voxels on images with different noise and bias field levels.

V. Experimental Results

We evaluate the results on both T_1-weighted synthetic and real 3D MR images. Synthetic images are with size 181 × 217 × 181 and voxel size 1 × 1 × 1 mm^3 from Montreal Neurological Institute [6] BrainWeb. Real images are with size 208 × 256 × 120 and voxel size 1 × 1 × 1.3 mm^3. Results are compared with the HMRF model [9] and/or the FGM model. We first experiment on synthetic brain MR images with known labels

for all tissues. Figure 4 shows the effect of different values of ω on images with different noise (%*N*) and different bias field level (%*RF*). The noise in the synthetic data has Rayleigh statistics in the background and Rician statistics in the signal regions. The "percent noise" number represents the percent ratio of the standard deviation of the white Gaussian noise versus the signal for a reference tissue. The *RF* level represents the bias field effect. For example, a 20% level RF means the multiplicative bias field has a range of values of 0.90 ... 1.10 over the brain area. The vertical axis is the accuracy improvement ratio of the RBHMRF model to the HMRF model on all voxels near the boundaries between different tissue types. The accuracy has apparent improvement in cleaner data with larger ω and small improvement in noisy data with smaller ω. It has negative effect when the noise is severe and ω is large. This is due to the corruption of the structure of the brain under severe noise. In such cases, using the characteristics of human brain structure becomes problematic. Figure 5 compares segmentation accuracy on the whole MR images of the FGM model, the HMRF model, and the RBHMRF model with best ω. The HMRF model is criticized with little improvement on cleaner data compared to the FGM model [4]. RBHMRF successfully solves this problem by considering the intrinsic structures of the brain. Figure 6 shows one slice of synthetic images with ground truth labels and the segmentation results. Next, we experiment on 10 real MR images and investigate the results. It can be seen that the RBHMRF model has better segmentation results on real data as well. Figure 7 shows two example slices of the segmentation results on real MR images.

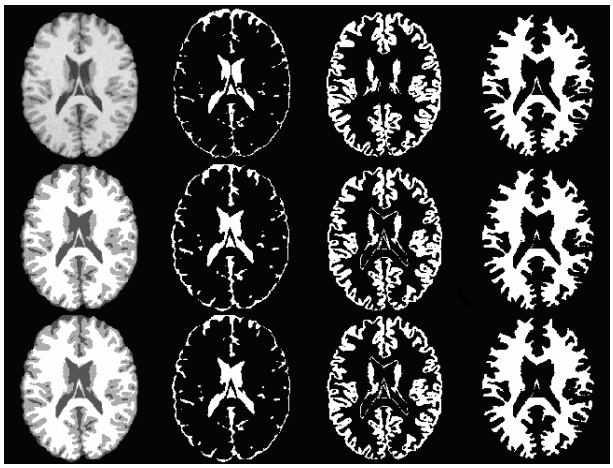

Fig. 6. Comparison of the segmentation results on synthetic data (3%N, 20%RF). 1st row: Original image, ground truth CSF, ground truth GM, ground truth WM, respectively. 2nd and 3rd rows: Segmentation results by HMRF, and RBHMRF (ω = 0.5).

VI. Discussion and Conclusion

In this paper, we propose the region-based hidden Markov random field model for brain MR image segmentation and illustrate its effectiveness. The improved accuracy rate according to the experimental results is due to better characterization of natural brain structure. Empirically, ω = 0.3 to 0.5 is a good setting for real MR images. For noisier data, ω should be set smaller. Besides, the TV+L^1 model is used for larger-scale region selection. Hidden Markov random field is used widely in many other image processing or pattern recognition applications. We believe the idea of using different regions with different weighting functions according to the characteristics of the data may be contributive to other applications as well. Our future work will be automatically and adaptively choosing the optimal ω based on the noise level of the image according to its intensity distribution.

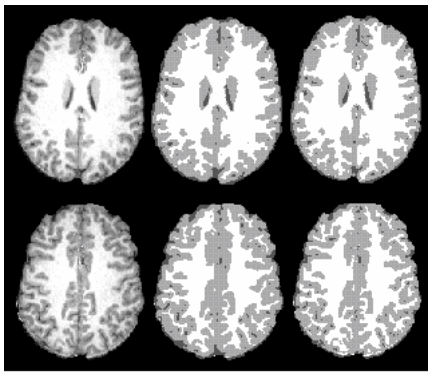

Fig. 7. Segmentation results on real data.

References

[1] J. Besag, Spatial interaction and the statistical analysis of lattice system (with discussion), J. of Royal Statist. Soc., series B, 36(2):192-326, 1974.
[2] T. F. Chan, and S. Esedoglu, Aspects of Total Variation Regularized L^1 Function Approximation" to appear in USIAMJ. Appl. Math. 2005.
[3] L. P. Clarke, R. P. Velthuizen, M. A. Camacho, J. J. Heine, M. Vaidyanathan, L. O. Hall, R. W. Hatcher, and M. L. Silbiger, MRI Segmentation: methods and applications, Megnetic Resonance Imaging, 13(3):343-368, 1995.
[4] M. B. Cuadra, B. Platel, E. Solanas, T. Butz, and J. -Ph. Thiran, Validation of tissue modelization and classification techniques in T1-weighted MR brain images, MICCAI, pp. 290-297, 2002.
[5] R. Guillemaud, and J. M. Brady, Estimating the bias field of MR images, IEEE Transactions on Medical. Imaging, 16(3):238-251, 1997.
[6] R. K. -S. Kwan, A. C. Evans, and G. B. Pike, MRI simulation-based evaluation of image-processing and classification methods, IEEE Transactions on Medical. Imaging, 18(11):1085-1097, Nov, 1999.
[7] E. Solanas, V. Duay, O. Cuisenaire, and J. -P.Thiran, Relative anatomical location for statistical non-parameter brain tissue classification in MR images, Int'l conference on image processing (ICIP), 2001.
[8] W. M. Wells, E. L. Grimson, R. Kikinis, and F. A. Jolesz, Adaptive segmentation of MRI data, IEEE Transactions on Medical. Imaging , 15(4):429-442, 1996.
[9] Y. Zhang, M. Brady, and S. Smith, Segmentation of brain MR images through a hidden Markov random field model and the expectationmaximization algorithm, IEEE Transactions on Medical. Imaging, 20(1):45-57, 2001.
[10] S. C. Zhu, and A. Yuille, Region Competition: Unifying snakes, region growing, and Bayes/MDL for multiband image segmentation, IEEE Transactions on Pattern Analysis and Machine Intelligence, 18(9):884-900, 1996.